AIP | Physics of Plasmas

Measuring preheat in laser-drive aluminum using velocity interferometer system for any reflector: Experiment

Hua Shu, Sizu Fu, Xiuguang Huang, Jiang Wu, Zhiyong Xie, Fan Zhang, Junjian Ye, Guo Jia, and Huazhen Zhou

Citation: Physics of Plasmas (1994-present) **21**, 082708 (2014); doi: 10.1063/1.4891429
View online: http://dx.doi.org/10.1063/1.4891429
View Table of Contents: http://scitation.aip.org/content/aip/journal/pop/21/8?ver=pdfcov
Published by the AIP Publishing

Measuring preheat in laser-drive aluminum using velocity interferometer system for any reflector: Experiment

Hua Shu, Sizu Fu, Xiuguang Huang, Jiang Wu, Zhiyong Xie, Fan Zhang, Junjian Ye, Guo Jia, and Huazhen Zhou
Shanghai Institute of Laser Plasma, P.O. BOX 800-229, Shanghai 201800, China

(Received 14 February 2014; accepted 14 July 2014; published online 14 August 2014)

In this paper, we systematically study preheating in laser-direct-drive shocks by using a velocity interferometer system for any reflector (VISAR). Using the VISAR, we measured free surface velocity histories of Al samples over time, 10–70 μm thick, driven directly by a laser at different frequencies (2ω, 3ω). Analyzing our experimental results, we concluded that the dominant preheating source was X-ray radiation. We also discussed how preheating affected the material initial density and the measurement of Hugoniot data for high-Z materials (such as Au) using impedance matching. To reduce preheating, we proposed and tested three kinds of targets. © *2014 AIP Publishing LLC*. [http://dx.doi.org/10.1063/1.4891429]

I. INTRODUCTION

Laser shock experiments are performed to create high pressures (>10 Mbars) in materials.[1–7] When a high energy laser irradiates a solid, its surface layers are converted into a plasma and a shock is generated and propagates into the target compressing it.

One of the most promising applications of lasers is their use in the equation of state measurements of materials at dynamic pressures much higher than that can be obtained by gas guns or explosives. Early work with lasers generated multimegabar shocks. Later work using direct and indirect drive reached much higher pressures over larger spot areas, and recently produced a startling result. These laser drives can reach pressure regimes in the laboratory only exceeded by nuclear weapons pressures and geophysical pressures. However, the same processes that allow generation of these high pressures also generate preheat in the targets that are being shocked or are being accelerated.[8–10] Preheating is a process in which the x rays (or hot electrons) generated in the plasma corona heat matter ahead of the laser shock. This preheat is serious issue, for it not only affects the initial state of the material we wish to study, it also causes a physical expansion of the material as well, making the measurement different from the typically desired on-Hugoniot conditions (also called principal Hugoniot, or the Hugoniot).

The measurement and understanding of preheat is important in equation of state (EOS) measurement with laser shocks. For the proper design and interpretation of laser-driven shock wave experiments, one needs to quantify the level of preheat in the material ahead of the shock front. Previous studies of preheating used different approaches. The emission of the target rear side has been recorded and the temperature estimated with the hypothesis of black body emission as brightness or color temperature.[11,12] Alternatively, the temporal shape of the signal (and in particular the appearance of an early emission before shock breakout) has been related to preheating. Recently, Benuzzi *et al.*[13] have studied preheating using the reflectivity of the target rear side.

In this paper, we systematically studied preheating in laser shocks by using a line-image velocity interferometer system for any reflector (VISAR).[14] The VISAR measures shock breakout times at temporal resolutions as low as 20 ps and at a spatial resolution of ~7 μm. The expansion velocity of the Al target backside was measured continuously by the VISAR. We characterized the preheating degree for different Al thicknesses using the magnitude of the free surface velocity. Preheating was studied with laser-direct-drive conditions of 2ω and 3ω. We also studied the relation between the preheating and target thickness, and we discussed how preheating affected the initial material density and measurement of Hugoniot data for high-Z materials (such as Au) using impedance-matching. To reduce preheating, we proposed three kinds of targets, finding that they all reduced preheating and that one completely eliminated preheating.

II. EXPERIMENTAL SETUP

This experiment was performed using the "Shenguang-II" Nd:glass laser of the National Laboratory on high power laser and physics. The "Shenguang-II" laser facility has nine laser beams. One of the nine beams is called "the ninth beam," which could output 3000 J laser energy. The temporal profile of the laser is nearly square with a rise and fall time of ~300 ps and a full width at half maximum (FWHM) of ~2.4 ns. The other eight beams could output 500 J with a pulse width of ~1 ns.

In the experiments, "the ninth beam" (converted to 2ω or 3ω) directly illuminated the target. The laser beam was smoothed using a lens-array system to eliminate large-scale spatial modulation and to obtain a flat-topped profile in the focal plane. Characteristics of the optical system (lens + LA)[15–17] were such that the focal spot had a ~1 mm diameter flat region. The peak laser irradiance on the target was $\sim 1.0 \times 10^{14}$ W/cm^2. A schematic view of the experimental configuration is shown in Figure 1. The free surface velocity histories of the aluminum sample (flat or multi-step) were obtained with a two-channel VISAR. The VISAR

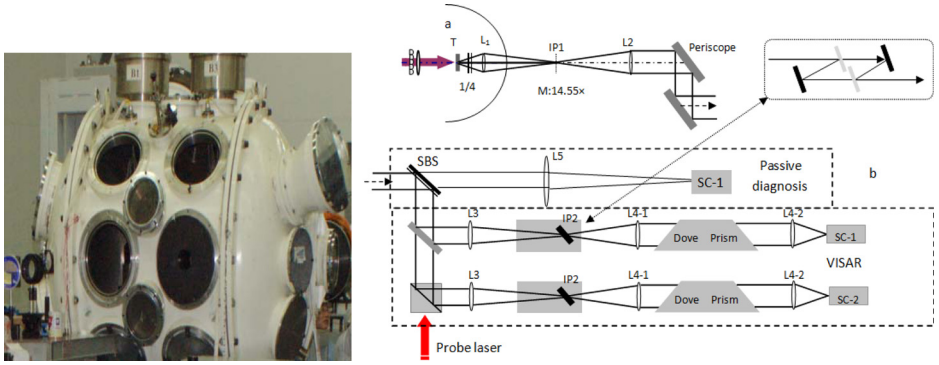

FIG. 1. The image on the left is a picture of the target chamber; The image on the right is the schematic of the diagnostic system (a).The first stage is a microscopic zoom imaging system with an intermediate image plane localized at IP1 (b). The beam from IP1 are recollimated by L2 and through a periscope system onto the optical table, where it reaches a special designed beam splitter (SBS) and imaged by L3 localized at IP2, the beam from IP2 are recollimated by $L_{4\text{-}1}$ and imaged by $L_{4\text{-}2}$ at the slit of the streak camera.

system had a temporal resolution of ~20 ps and a spatial resolution of ~7 μm.

III. EXPERIMENTAL RESULTS

A. 3ω laser-drive experiment

In this experiment, the drive laser was converted to the third harmonic (3ω) and directly illuminated the target. The VISAR recorded the free surface velocity history and reflectivity of rear side of the target.

Figure 2 (left plot) shows an image obtained with the VISAR (drive laser frequency is 3ω, the measured laser energy is 2150 J at 1ω). The horizontal direction in the image is space, and the vertical direction is time. The temporal scale of the image is 2 ns. The thickness of the Al flat target was 30 μm. The length of the etalon was 60 mm, corresponding to a fringe constant of 0.9 km/s/fringe. The interference fringes moved before shock breakout, demonstrating that the target was preheated by X-rays or hot electrons. Figure 2 (right plot) shows the free surface velocity history. The maximum expansion free surface velocity was ~1.2 km/s. To study the relation between preheating and target thickness, we used an Al multi-step target, configuration as shown in Figure 3(a). The parameters of this target were $S_1 = 10\ \mu$m, $S_2 = 30.5\ \mu$m, and $S_3 = 20.3\ \mu$m. Figure 3(b) shows a VISAR image of the multi-step target (shot 1). The drive laser energy was 1952 J (1ω). Figure 3(c) shows profiles of the free surface velocity for shot 1. Figure 4(a) shows a VISAR image of a second experiment with nearly the same drive laser energy (shot 2). The parameters of this target were $S_1 = 20\ \mu$m, $S_2 = 30.5\ \mu$m, and $S_3 = 20.8\ \mu$m. Figure 4(b) shows profiles of the free surface velocity for shot 2. These experiments revealed that the free surface velocity decreased as the Al thickness increased. Table I shows the expansion distance for different Al thicknesses. The Al thickness changed from expansion of the free surface, which would significantly affect measurements of Hugoniot data of high-Z materials, such as Au, using impedance-match method. This will be discussed in Sec. III D.

B. 2ω laser drive experiment

In this experiment, the drive laser was converted to the second harmonic (2ω) and directly illuminated the target. An Al step-target was used, as in Sec. III A. The base thickness of the step-target was 30 μm. The step thickness was 15 μm. Figure 5 shows VISAR images of the Al step-target at different drive laser energy. The experimental results show that the free surface velocity increased with the increasing of driving laser energies. Figure 6 compares the measured free surface velocities of the 2ω and 3ω laser drive conditions. The laser irradiance on the target was nearly same. The free surface velocity profile of the 50 μm Al flat, driven by the 3ω laser, is shown by the black line, the free surface velocity profile of the 45 μm Al flat, driven by the 2ω laser, is shown by the red line.

C. Preheat reduction

In this experiment, the drive laser was converted to the third harmonic (3ω) and directly illuminated the target. To

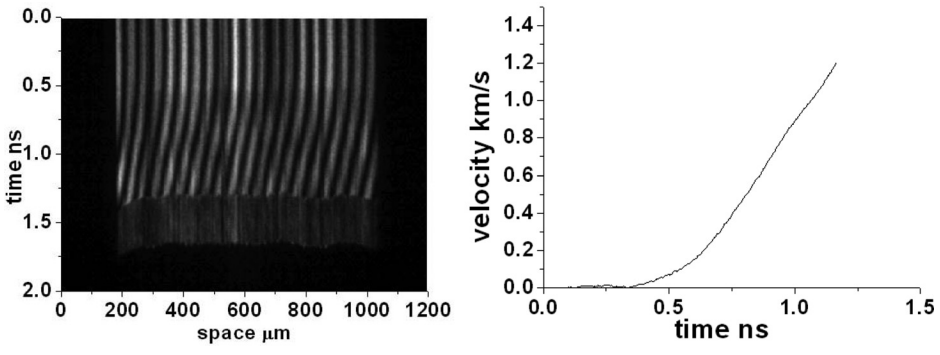

FIG. 2. Experimental result, the laser was converted to 3ω; the first plot on the left shows the VISAR image. The right plot shows the free surface velocity obtained from the VISAR.

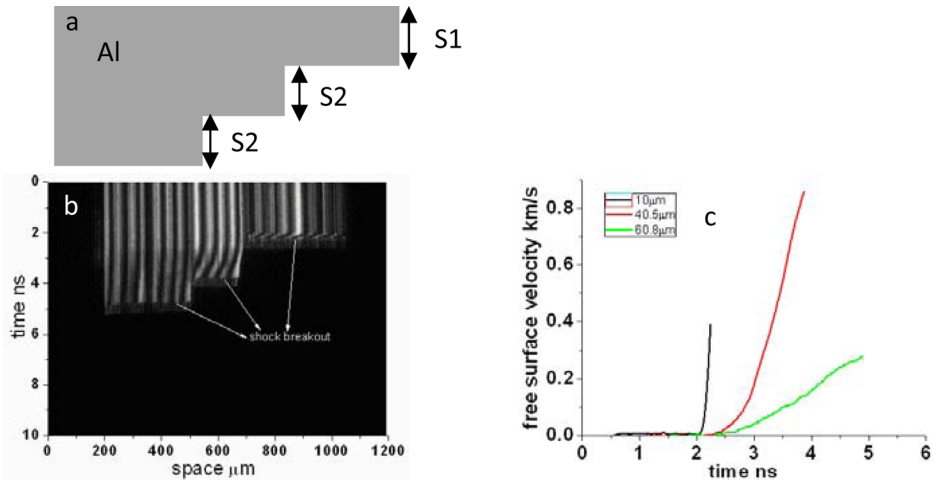

FIG. 3. Experimental results of a multi-step target, the drive laser was converted to 3ω; (a) Target configuration, S1 = 10 μm, S2 = 30.5 μm, S3 = 20.3 μm; (b) VISAR image; (c) Free surface velocity of different thickness of Al samples.

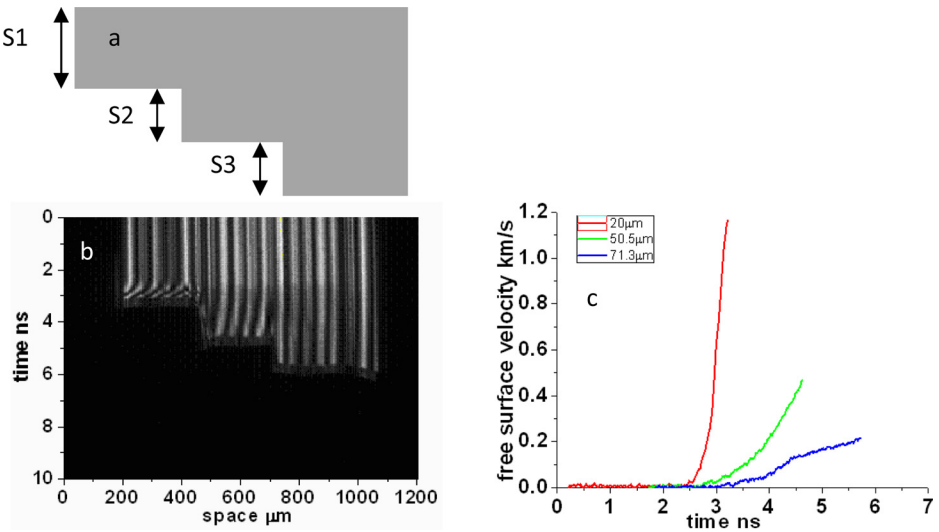

FIG. 4. Experimental results of a multi-step target, the drive laser was converted to 3ω; (a) target configuration, S1 = 20 μm, S2 = 30.5 μm, S3 = 20.8 μm; (b) VISAR image; (c) free surface velocity of different thickness of Al samples.

reduce preheating, we proposed three kinds of targets, configured as shown in Fig. 7. The first target (Fig. 7(a)) consisted of 5 μm Al, 0.9/1.5 μm Au, and 25 μm Al. The Au film acts as a preheating shield by absorbing X-rays formed in the laser ablation region at the front of the target. The second target (Fig. 7(b)) consisted of 30 μm polystyrene ablator and 30 μm Al. The third target (Fig. 7(c)) consisted of 10 μm polystyrene ablator, 20 μm 2.8% brominated polystyrene ($C_{50}H_{47.2}Br_{2.8}$), 30 μm Al base, and 9.5 μm Al step. The bromine dopant shielded against preheating by absorbing X-rays formed in the laser ablation region at the front of the target

Figure 8 shows VISAR images of the configuration of the first target with 0.9 μm and 1.5 μm thick Au preheat shields. The drive laser was converted to 3ω. The measured laser energy was nearly 2000 J (1ω). The Au shield significantly reduced the preheat, but the preheat could not be completely suppressed using the 1.5 μm Au preheat shield. To completely suppress the preheat, we increased the Au thickness. When the Au shield was 5 μm thick, the VISAR image revealed no fringe shift before shock breakout. Figure 9 shows a VISAR image of the configuration of the second target. The drive laser was converted to 3ω. The measured laser energy was nearly 2000 J (1ω). The maximum free surface velocity was ~0.32 km/s. These results revealed that the CH ablator reduced preheating relative to the Al ablator. Figure 10 shows a VISAR image of configuration of the third target. The drive laser was converted to 3ω. The measured laser energy was nearly 2500 J (1ω). The VISAR image revealed no fringe shift before shock breakout, showing that there was little to no preheat.

TABLE I. Expansion distance of different thickness Al samples.

Al height (μm, d)	20	30	40	50	60	70
Expansion distance (μm, Δd)	0.3	0.49	0.48	0.32	0.31	0.28
Thickness deviation (Δd/d)	1.5%	1.6%	1.2%	0.64%	0.52%	0.4%

D. Discussion

1. Preheating source

Here, we will discuss the preheating source of the 3ω laser- drive condition based on the experimental results. The source of preheating is X-ray radiation and electron heat transport in laser drive shock wave experiments. Our results show that the depth of Al affected by preheating was ~70 μm. If we assume that the main source of preheating is

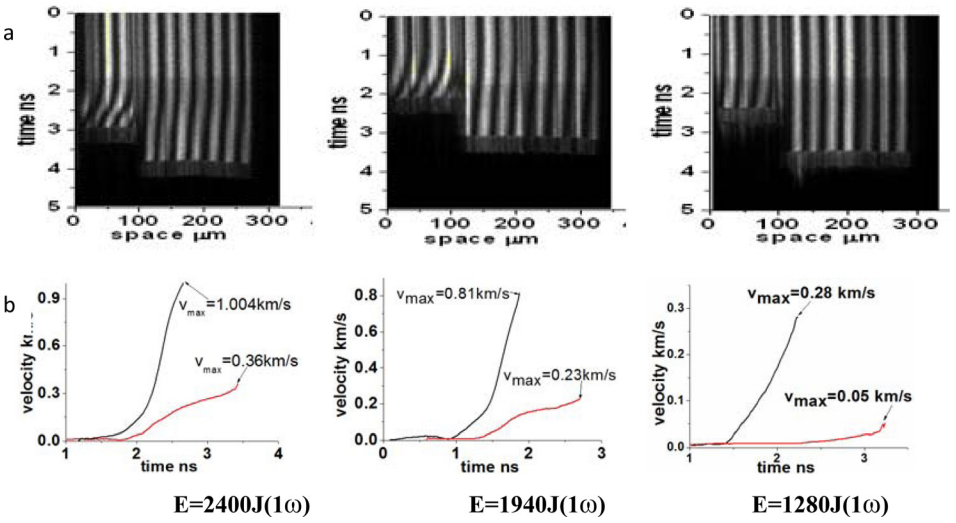

FIG. 5. (a) VISAR images of the Al step-target with different laser energy (the laser was converted to 2ω); (b) free surface velocity obtained from Fig. 5(a).

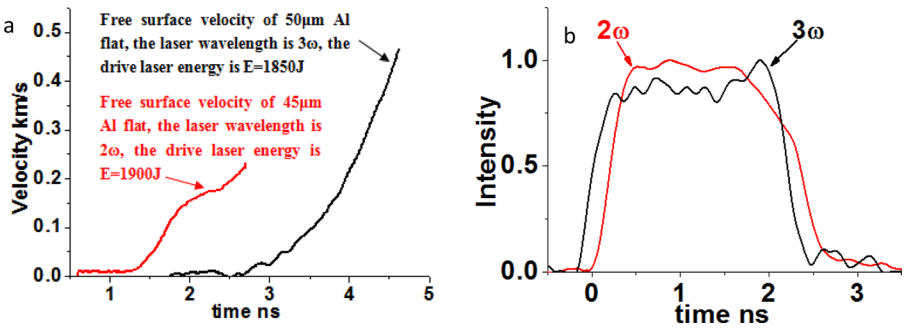

FIG. 6. (a) A comparison of the measured free surface velocity of the 2ω laser drive condition and the 3ω laser drive condition. The laser irradiance on the target is nearly same; the free surface velocity of 50 μm Al flat drive by the 3ω laser was shown in black line; the free surface velocity of 45 μm Al flat drive by the 2ω laser was shown in red line. (b) The measured pulse shape of the drive laser; The measured laser irradiance is about $\sim 6.5 \times 10^{13}$ W/cm^2.

hot electrons, we can estimate the electron energy according to the empirical formula for electron transport range in an Al medium $(\mathrm{d}(\mu\mathrm{m}) = \frac{4.12\times10^3}{\rho_{\mathrm{Al}}}\mathrm{E}^{(1.265-0.0954\ln\mathrm{E})})$.[18,19] Using this empirical formula with a transport range of 70 μm, we estimated the energy of the hot electron to be 122.4 KeV. However, our result shows that a 1.5 μm Au shield effectively reduced preheating. Using the empirical formula of electron transport range in a Au medium $\mathrm{d}(\mu\mathrm{m}) = \frac{0.19}{\rho_{\mathrm{Au}}}\mathrm{E}^{1.6}$,[18] we found that hot electrons with energies of $<$23.4 KeV could be blocked by a 1.5 μm Au shield. The two conclusions from these two equations are contradict each other, so we conclude that the main preheat source of the 3ω laser-drive condition was X-ray radiation.

2. Dependence of preheat on material initial density and shock velocity

Here, we will discuss how the preheating affected the material initial density and shock velocity.

The focal spot of the drive laser on the target is a rectangle with a long side of $\mathrm{L1} = 1$ mm and a short side of $\mathrm{L2} = 0.7$ mm. The target thickness d was on the order of tens of microns. The initial sample volume was $\mathrm{V0} = \mathrm{L1} \times \mathrm{L2} \times \mathrm{d}$. The sample volume after preheating is $\mathrm{V} = (\mathrm{L1} + \Delta\mathrm{d}) \times (\mathrm{L2} + \Delta\mathrm{d}) \times (\mathrm{d} + \Delta\mathrm{d})$, where Δd is the free surface expansion distance. From our experimental results, the expansion distance Δd was a few tens of microns, so the sample volume was $\mathrm{V} \approx \mathrm{L1} \times \mathrm{L2} \times (\mathrm{d} + \Delta\mathrm{d})$. The sample density after reheating can be expressed as $\frac{\rho}{\rho_0} = \frac{\mathrm{v}_0}{\mathrm{v}} \approx 1/(1 + \Delta\mathrm{d}/\mathrm{d})$. Using the results from shot 1, we can estimate how the preheating affected the initial density. The initial target thickness was 20 μm, and the measured free surface expansion distance Δd was $\sim$0.3 μm. Thus, the density ρ after preheating was 2.67 g/cm^3, and $\frac{\Delta\rho}{\rho_0} \approx 1.5\%$ (assuming an initial Al density of 2.71 g/cm^3). Next, we could estimate the effect of the density decrease on the shock velocity. Based on the Rankine-Hugoniot conservation relation, one can obtain $\mathrm{P} - \mathrm{P}_0 = \rho_0(\mathrm{D} - \mathrm{u}_0)(\mathrm{u} - \mathrm{u}_0)$, where P, ρ, D, and u are the pressure, density, shock velocity, and particle velocity, respectively. The zero subscripts denote the initial material condition ahead of the shock front. The relation could be simplified to the form $\mathrm{P} = \rho_0 \mathrm{D}\mathrm{u}$, which is physically meaningful since it implies $\mathrm{u}_0 = 0$ at $\mathrm{p}_0 = 0$. The relation between D and u of Al was practically linear, $\mathrm{D} = \mathrm{C} + \mathrm{S}\mathrm{u}$, where

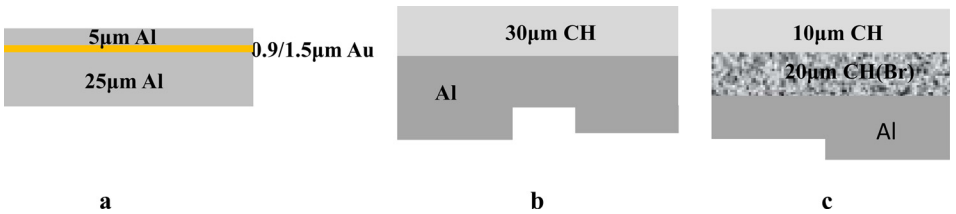

FIG. 7. Target configuration; (a) 5 μm Al ablator, 0.9 or 1.5 μm Au preheat shield and 25 μm Al flat; (b) 30 μm CH ablator, 30 μm Al base and two Al step; (c) 10 μm CH ablator, 20 μm 2.8% CH (Br) preheat shield, 30 μm Al base and 9.5 μm Al step.

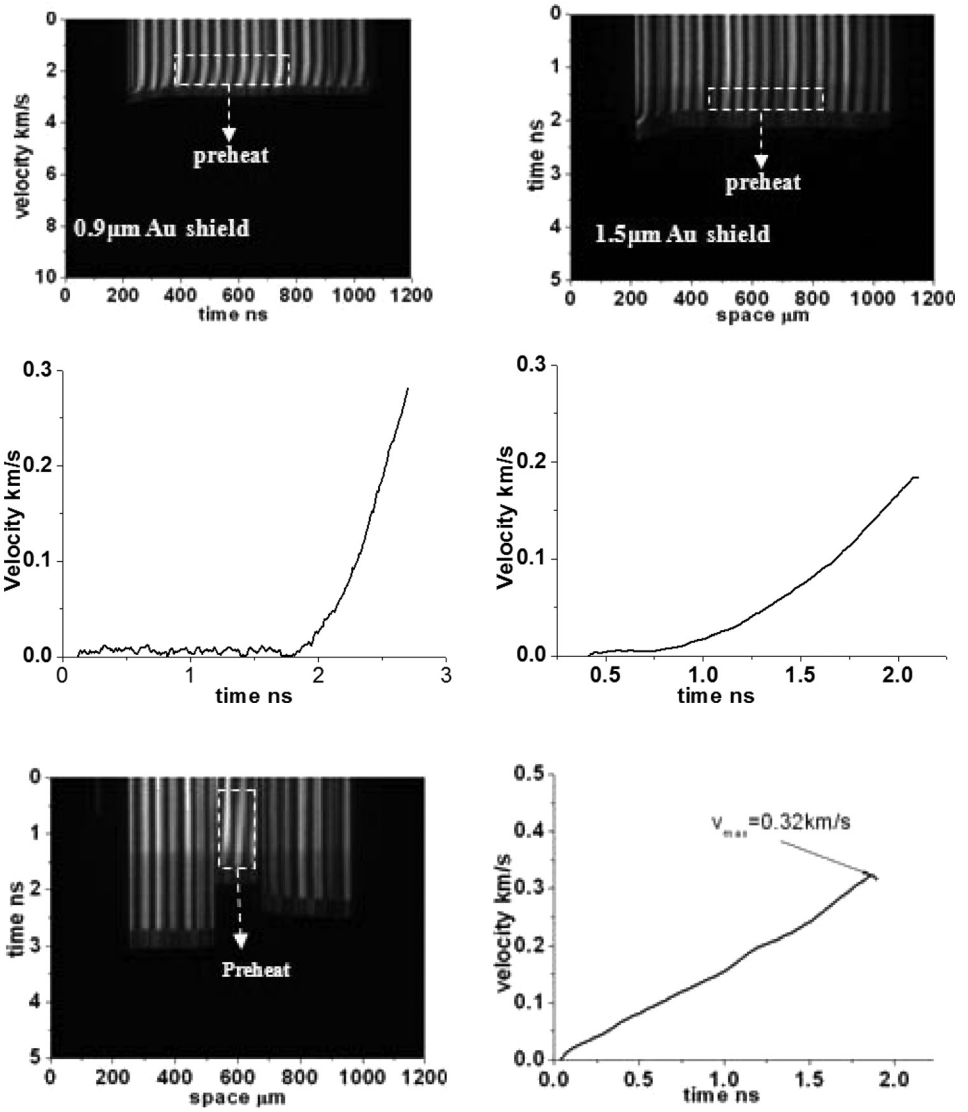

FIG. 8. Experimental results of the target configuration (a) with different thickness of Au shield (the drive laser was converted to 3ω, the drive laser energy is about 2000 J (1ω)); the plot on top is the VISAR image. in the left image, the Au shield thickness is 0.9 μm; in the right image, the Au shield thickness is 1.5 μm; at the bottom, the plots present the free surface velocity.

FIG. 9. The VISAR image and the free surface velocity of the target configuration (b), the drive laser energy was nearly 2000 J (the drive laser was converted to 3ω).

C $\approx$ 5.89 km/s is the order of the sound velocity in the material and S $\approx$ 1.2. At a fixed pressure, one can obtain $\frac{dD}{D} = \frac{d\rho_0 u}{-\rho_0(u+D\frac{\partial u}{\partial D})}$ from the relation $P = \rho_0 Du$. Using the linear relation of D and u, one can obtain $\frac{dD}{D} = \frac{d\rho_0}{-\rho_0}\frac{(D-C)}{(2D-C)}$. Using the results of shot 1, we can estimate the effect of the density decrease on the shock velocity. The measured shock velocity of Al was D = 19.93 μm/ns. The estimated density change was $\frac{\Delta\rho}{\rho_0} \approx 1.5\%$. So, the shock velocity change was $\sim\frac{dD}{D} \approx 0.62\%$.

3. Effect of preheating on Hugoniot data measurement

Here, we will discuss how the preheating affected the measurements of Hugoniot data for high-Z materials (such as Au) using impedance-match method. A typical

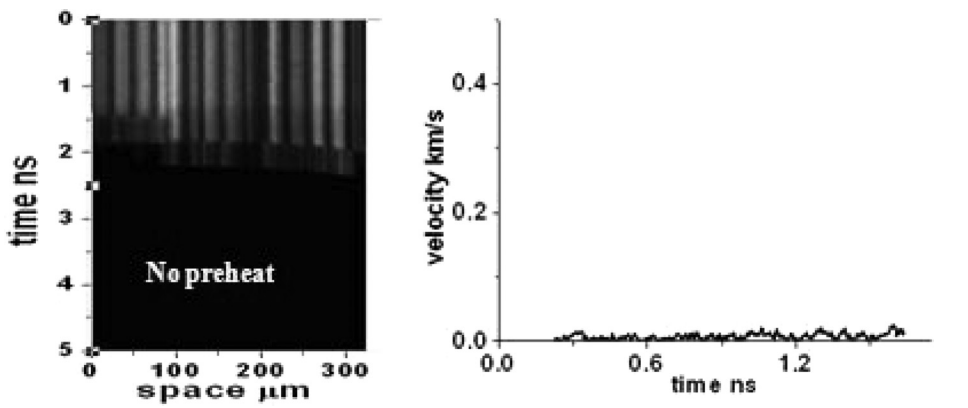

FIG. 10. The VISAR image and the free surface velocity of the target configuration (c); the drive laser energy is nearly 2500 J (the drive laser was converted to 3ω).

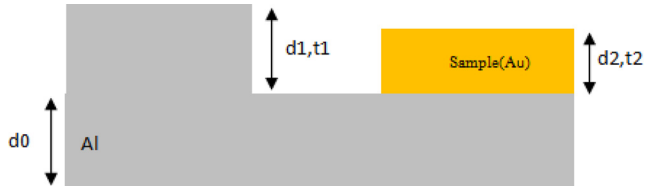

FIG. 11. Schematic of a typical impedance-match target; d1 and d2 is the thickness of standard and unknown material. t1 and t2 are the shock wave propagation time.

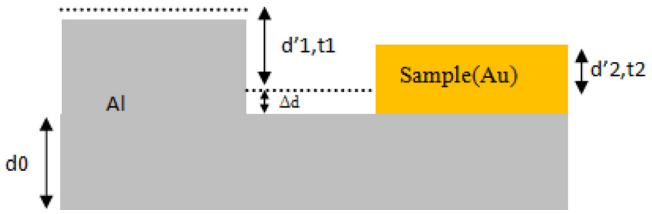

FIG. 12. Schematic of the impedance-target after it is preheated.

impedance-match target is shown in Figure 11. Before the experiments, we measured the step heights d1 and d2 using a white-light interferometer. The shock propagation times t1 and t2 were measured using a streak camera. The measured shock velocity D1 = d1/t1 and D2 = d2/t2 could be obtained on the same shot.

Figure 12 shows the target after preheating. Preheating caused the Al free surface to expanded to the position shown by the dashed line. The free surface of the Au sample remained motionless. The true measured shock propagation times t1 and t2 correspond to the shocks transmitted in d'1 and d'2. The actual shock velocities are D'1 = d'1/t1 and D'2 = d'2/t2. From the results of the multi-step target experiment, the relationship between d'1 and d1 is uncertain, causing dispersion in the measurement of the shock velocity a standard material. The thickness d'2 is always less than d2, causing systematic bias on the shock velocity measurements of an unknown sample. Now, using the experimental results of shot 1, we can estimate how preheating affected the measurements of the sample shock velocity. The Al base d0 was 20 μm, The Al step d1 was 30.5 μm, and we assumed the Au thickness to be 5 μm.

The measured shock propagation time in the Al step (S2 = 30.5 μm) was t1 = 1.53 ns, so the measured shock velocity was D1 = 30.5 μm/1.53 ns = 19.93 μm/ns. The true shock velocity was D'1 = (30.5 − 0.3 + 0.32) μm/1.53 ns = 19.95 μm/ns, where 0.3 μm and 0.32 μm are the expansion distance of the Al base and Al step. The difference between the true and measurement shock velocities is very small. For an Au thickness is of 5 μm and a shock propagation time in the Au step of t2, the measured shock velocity is D2 = 5 μm/t2. The actual shock velocity is D'2 = (5 − 0.3) μm/t2. The difference between the measured and the actual shock velocity is (D2-D'2)/ D2 = 6%, which seriously affects measurements of Hugoniot data.

IV. CONCLUSION

A systematic study of preheating in laser direct-drive shocks was performed. We indirectly characterized the preheating degree by using the free surface velocity, measured using VISAR. Our experimental results showed significant preheating in the laser direct-drive shock wave experiments. We also studied the relationship between preheating and the target thickness.

From our experimental results, we concluded that the dominant source of preheating was X-ray radiation. We found that target density barely affected by preheating. We also discussed how preheating affected the measurements of Hugoniot data of High-Z materials (such as Au) using impedance-matching. We found that preheating significantly affected the measurement of shock velocity for an unknown sample. Preheating will cause systematic bias in measurements of shock velocity.

We proposed three kinds of target configurations to reduce preheating. We found that preheating was completely suppressed by using the CH ablator and a CH (Br) preheat shield.

ACKNOWLEDGMENTS

This work was supported by the 863 National High-tech Plan of the People's Republic of China. The authors also gratefully acknowledge the valuable experimental support by the technical crews of "Shenguang-II."

[1]A. Benuzzi, T. Löwer, M. Koenig, B. Faral, D. Batani, D. Beretta, C. Danson, and D. Pepler, "Indirect and direct laser driven shock waves and applications to copper equation of state measurements in the 10–40 Mbar pressure range," Phys. Rev. E **54**, 2162 (1996).
[2]D. Batani, A. Morelli, M. Tomasini, A. Benuzzi, F. Philippe, M. Koenig, B. Marchet, L. Masclet, M. Rabec, Ch. Reverdin, R. Cauble, P. Celliers, G. Collins, L. Da Silva, T. Hall, M. Moret, B. Sacchi, P. Baclet, and B. Cathala, "Equation of state data for iron at pressures beyond 10 Mbar," Phys. Rev. Lett. **88**, 235502 (2002).
[3]D. Batani, F. Strati, H. Stabile, M. Tomasini, G. Lucchini, A. Ravasio, M. Koenig, A. Benuzzi, H. Nishimura, Y. Ochi, J. Ullschmied, J. Skala, B. Kralikova, M. Pfeifer, Ch. Kadlec, T. Mocek, A. Präg, T. Hall, P. Milani, E. Barborini, and P. Piseri, "Hugoniot data for carbon at megabar pressures," Phys. Rev. Lett. **92**, 065503 (2004).
[4]D. Batani, A. Balducci, D. Beretta, A. Bernardinello, T. Löwer, M. Koenig, A. Benuzzi, B. Faral, and T. Hall, "Equation of state data for gold in the pressure range <10 TPa," Phys. Rev. B **61**, 9287 (2000).
[5]S. D. Rothman, A. M. Evans, C. G. Horsfield, P. Graham, and B. R. Thomas, "Impedance match equation of state experiments using indirectly laser-driven multimegabar shocks," Phys. Plasmas **9**, 1721 (2002).
[6]D. G. Hicks, T. R. Boehly, P. M. Celliers, J. H. Eggert, E. Vianello, D. D. Meyerhofer, and G. W. Collins, "Shock compression of quartz in the high-pressure fluid regime," Phys. Plasmas **12**, 082702 (2005).
[7]N. Ozaki, K. A. Tanaka, K. O. T. Shigemori, M. Nakai, H. Azechi, and T. Yamanaka, "GEKKO/HIPER-driven shock waves and equation-of-state measurements at ultrahigh pressures," Phys. Plasmas **11**, 1600 (2004).
[8]D. Batani and F. Giugliano, "Interferometric measurement of preheating in laser shocks," Phys. Rev. E **64**, 047401 (2001).
[9]D. K. Bradlesy, S. T. Prisbrey, R. H. Page, D. G. Braun, M. J. Edwards, R. Hibbard, K. A. Moreno, M. P. Mauldin, and A. Nikroo, "Measurements of preheat and shock melting in be ablators during the first few nanoseconds of a national ignition facility ignition drive using the omega laser," Phys. Plasmas **16**, 042703 (2009).
[10]G. A. Kyrala, R. P. Johnson, and T. Hurry, "A new interferometer to measure preheat in laser targets," Rev. Sci. Instrum. **70**, 682 (1999).
[11]Th. Lower, R. Sigel, K. Eidmann, L. B. Földes, S. J. Massen, G. D. Tsakiris, S. Witkowski, W. Preuss, H. Nishimura, H. Shiraga, Y. Kato, S. Nakai, and T. Endo, "Uniform multimegabar shock waves in solids driven by laser-generated thermal radiation," Phys. Rev. Lett. **72**, 3186 (1994).
[12]T. Hall, A. Benuzzi, D. Batani, D. Beretta, S. Bossi, B. Faral, M. Koenig, J. Krishnan, T. Löwer, and M. Mahdieh, "Color temperature measurement in laser-driven shock waves," Phys. Rev. E **55**, R6356 (1997).

[13]A. Benuzzi, M. Koenig, B. Faral, J. Krishnan, F. Pisani, D. Batani, S. Bossi, D. Beretta, T. Hall, S. Ellwi, S. Hüller, J. Honrubia, and N. Grandjouan, "Preheating study by reflectivity measurements in laser-driven shocks," Phys. Plasmas **5**, 2410 (1998).
[14]H. Shu, S. Z. Fu, X. G. Huang, J. Wu, H. Z. Zhou, and J. J. Ye, "A modified illumination system for a line-imaging optically recording velocity interferometer and its application in equation of state measurement," Meas. Sci. Technol. **23**, 015203 (2012).
[15]X. M. Deng, X. C. Liang, and Z. Chen, "Uniform illumination of large targets using a lens array," Appl. Opt. **25**, 377 (1986).
[16]H. Shu, S. Z. Fu, X. G. Huang, M. X. Ma, J. Wu, J. J. Ye, J. H. He, Y. Gu, P. Q. Luo, and T. Long, "Laser-driven shock wave stability in Al through Au and determination of the TPa hugoniot point in Au," J. Appl. Phys. **103**, 093304 (2008).
[17]H. Shu, S. Z. Fu, X. G. Huang, Z. H. Fang, T. Wang, J. J. Ye, Z. Y. Xie, H. Z. Zhou, and T. Long, "Laser-driven shock propagation into quartz targets driven by various drive pulse configurations: Experiments," Eur. Phys. J. D. **66**, 268 (2012).
[18]R. D. Evans, The Atomic Nucleus, 1955.
[19]R. J. Harrach and R. E. Kidder, UCRL-84846, 1980.